Transient and Residual Stresses in Multi-Pass Welds†

Yukio UEDA*, Eiji TAKAHASHI, Keiji FUKUDA*** and Keiji NAKACHO*****

Abstract

In order to examine the mechanical behavior of a multi-pass weld connection of a pressure vessel during welding (167 passes), theoretical and experimental investigations were conducted on an idealized research model. Theoretical thermal elastic-plastic analysis was carried out with the aid of a method developed by one of the authors, based on the finite element method.

Theoretically predicted residual stresses show very good concidence with those obtained from the experiment, thus, the highest longitudinal stress always appears below the surface of the latest layer, and in the residual stress distribution, the highest stress is produced several layers below the finishing bead in the midsection. Accordingly, when delayed cracking occurs, it initiates below the finishing bead and propagates to the surface.

1. Introduction

When thick plates are connected, it is usual to apply a multi-pass welding process. Although there have been many studies reported on weld cracks in multi-pass welds, it is very difficult to find information concerning detailed mechanical behavior of multi-weld joints in the entire course of welding. The main reason can be attributed to difficulties encountered in both theoretical analysis and experimentation[1]

Since one of the authors has developed an analytical method of thermal elastic-plastic problems solving based on the finite element method[2] (APPENDIX) the difficulties in theoretical analysis were fundamentally resolved and the application of this method has provided useful information on the mechanical behaviors of weld joints of many types[1), 3), 4)]

In this paper, an investigation[5] was carried out into welding stresses and strains induced in multi-pass welds in a research model (total 167 passes) the theoretical analysis was performed by the developed method, in which changes in the mechanical properties due to thermal cycles can be accounted with consideration of metallugical changes. An experiment was also conducted to be compared with theoretical analysis.

2. Research Model

In pressure vessels, there are many types of weld connection. In this study, a joint under conideration is that which lies between the cylinder and panel of a vessel, as shown in **Fig. 1,** where the angular

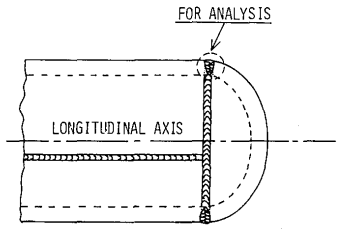

Fig. 1. Welded connections of pressure vessel.

distortion by thermal expansion and shrinkage is highly restrained and the axial displacement is almost free to move. The joint is idealized as illustrated in **Fig. 2** with due consideration preserving the fundamental character of the joint during welding as much as possible. The model is biaxially symmetric with respect to x- and y-axes. When each pass of weld is laid simultaneously on both sides of grooves, the angular distortion is prevented by the symmetry of the model. In this way, the restraining condition of the model is shown clearly and simply for theoretical analysis and experimentation and this does not require any special restraining instrumentation. In each side of groove, 83 passes of weld metal were laid.

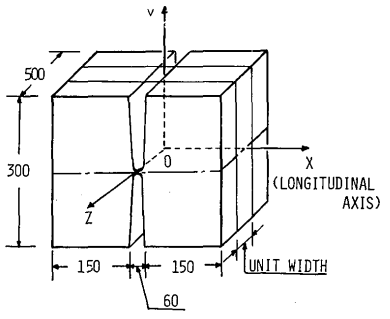

Fig. 2. Research Model.

† Received on Dec. 22, 1973
* Associate Professor
** Senior Researcher, Central Research Laboratory, Kobe Steel Ltd.
*** Graduate Student, Osaka University

3. Experiment

The base metal of the model was ASTM A336GF22 ($2\frac{1}{4}$ Cr—1 Mo) and the wire used for welding, US521XG80. Their chemical compositions are shown in **Table 1.**

In the study, two kinds of experiments were performed as indicated below:

(1) A test on the mechanical properties of the materials within a temperature range between 15℃ and 1000°C.

(2) A measurement of residual stresses in the model induced by multilayered welds.

Table 1. Chemical compositions of base and weld metals (%).

	C	Si	Mn	P	S	Cr	Mo
Base plate	0.09	0.29	0.46	0.04	0.013	2.38	1.03
Weld metal	0.07	0.42	0.78	0.012	0.012	2.28	1.06

3.1 Mechanical properties of metals

For the theoretical analysis, detailed information about the temperature dependent mechanical properties of the material was required, such as the modulus of elasticity, yield stress, linear thermal expansion coefficient, etc.

In the test, specimens were given a similar thermal cycle to that observed in the vicinity of the weld metal (Fig. 3). Based on the test results, the mechanical properties were determined for theoretical analysis. This will be defined in the following chapter.

3.2 Measurement of residual stresses in multilayered welds

The test model was subjected to multi-pass welds by sub-merged welding, and the welding condition is indicated in **Table 2.** Three passes of welding produced one layer as a standard procedure and every pass was laid on at the peak temperature of 200°C.

The measurement of residual stresses was made by the sectioning method after the model had cooled down. By sectioning the model into small pieces using a saw, the residual stresses were released. The released stresses were evaluated regarding differences of corresponding elastic strains between before and after sectioning. The elastic strains were measured by wire strain gauges put on the model. The residual stresses are represented in Fig. 7 for comparison with the theoretical results which will be furnished in the following chapter.

Table 2. Welding condition.

current	voltage	velocity	heat-input	preheating temperature
600 A	35 V	28 cm/min.	45000 J/cm	200°C

4. Theoretical Analysis of Residual Stresses by FEM

The behavior of the model during multi-pass welding is so complicated that theoretical analysis had to be performed with the aid of the finite element method, a developed method of thermal elastic-plastic analysis based on the finite element method including the temperature-dependent mechanical properties of metal[2].

In this study, the effect of coupling between temperature and stress fields is so small as to be negligible for such problems as welding. Moreover, the analysis can be divided into two separate parts: heat conduction analysis and stress analysis based on

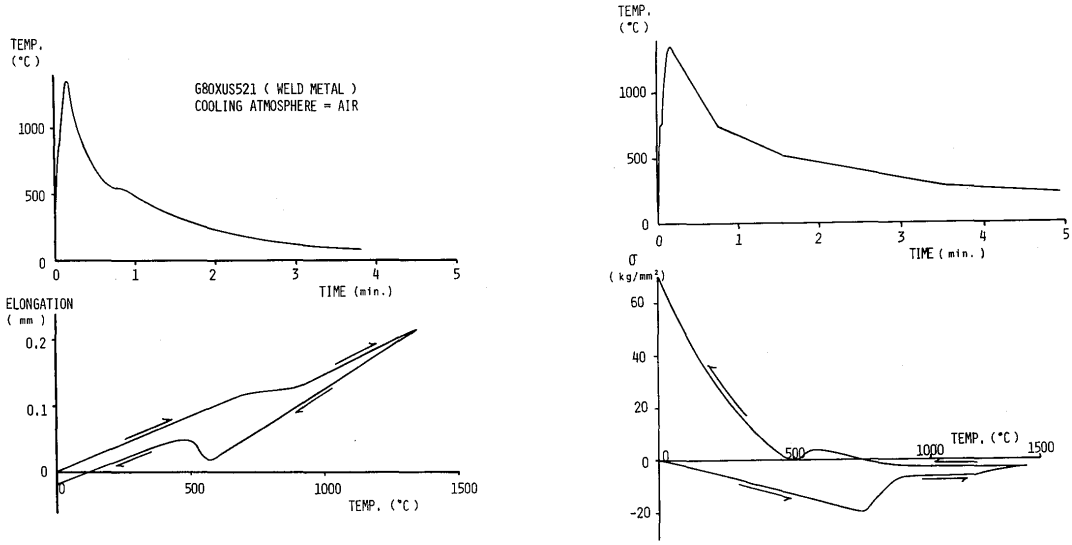

Fig. 3. Mechanical properties during thermal cycles

temperature distributions calculated in the preceding heat conduction analysis.

For both analysis, the physical and mechanical properties of base and weld metals were necessary. These properties were determined from test results obtained in addition to information already available.

4.1 Heat conduction analysis

In welding, heat conduction is not stationary, and heat transfer from the surface of the model has to be taken into account, since temperatures are very high and changes are rapid, immediately after the weld metal is laid. For the analysis, the finite difference method was applied dividing the model into small triangular meshes which were also used for the following stress analysis by the finite element method. The properties used in the analysis are assumed as shown in **Fig. 4** by which the size of the heat affected zone evaluated by the analysis is approximately the same as that observed in the test result.

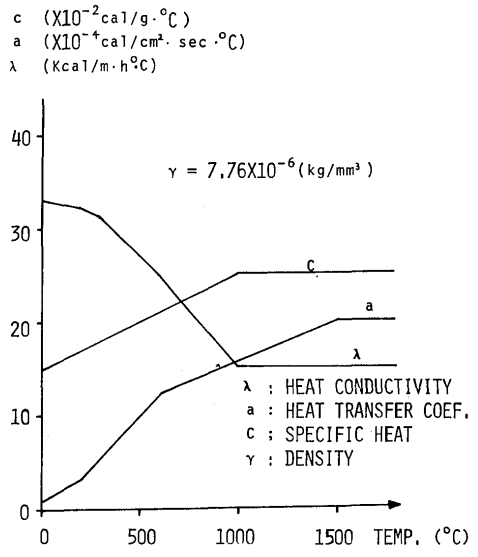

Fig. 4. Physical properties of the metal for theoretical analysis.

4.2 Residual stress analysis

Residual stress analysis was performed by the developed method of thermal elastic-plastic analysis. Accordingly, residual stresses were obtained as the resulting stresses in the thermal transient stress analysis.

In order to conduct the analysis, the mechanical properties of metal had to be specified.

It is a well-known fact that the stress-strain relationship of metal is influenced by many factors such as plastic strain history, strain rate, thermal cycle, etc. The linear thermal expansion coefficient is also dependent upon temperature, cooling rate, etc. especially during the transformation of phase of the material. It is almost impossible to obtain complete information on the mechanical properties of the metal under all possible welding condition in welding. For theoretical analysis, the stress-strain relationship and the linear thermal expansion coefficient are determined and idealized on the basis mentioned in Section 3.1. The thermal cycles which the material was subjected to were divided into two, the heating and cooling stages. The heating stage is further separated by whether the metal experiences above or below the phase transformation temperature of 750°C. In the analysis, two kinds of metal were treated, such as base and weld metals. The heat affected zone was regarded and later treated like the weld metal.

Based on the test results, it was determined that the Austenite phase transformation at the heating stage starts at a temperature of 750°C which corresponds to A_1, and the Martensite phase transformation, at a temperature of 600°C, that is, M_s. At higher temperatures than those of the transformations, both metals revealed no tendency to show resistance and then the thermal expansion and shrinkage accompanied by the transformations did not affect resulting stresses.

Both base and weld metals were treated as an elastic perfectly plastic material, since only a limited portion is subjected to large plastic strain at high temperatures, where the effect of strain-hardening is small.

Based on the above discussion, the mechanical properties of the metals were determined as illustrated in **Fig. 5.**

Actual computation was carried out accumulating each layer of weld in the grooves at the peak temperature of 200°C. Changes in temperature distribution were computed in the previous section and these produced stresses and strains in the thermal stress analysis. According to preliminary calculation, two layers of actual weld can be regarded as one layer in the analysis without loss of accuracy, since results of both computations are almost coincident.

Results of the analysis are shown in **Figs. 6** and **7. Figure 6 (a)** illustrates transient longitudinal stresses (in the x direction) on the surface at the peak temperature of 200°C in the intermediate processes of multilayer weld; and **Fig. 6 (b),** transient longitudinal stresses distributed in the y direction. The highest stress always appeared just below the surface of the latest layer. **Fig. 7 (a)** shows residual longitudinal stresses on the surface, the highest stress being produced approximately 20 mm away from the toe of the final bead. In **Fig. 7 (b),** residual longitudinal stresses induced along the y axis are indicated.

As seen in the figures, the highest longitudinal stress appears several layers below the bead surface where stress is positive but small. Judging from the residual stress distribution, delayed cracking would initiate below the finishing bead and propagate to the surface. The residual stresses obtained by the analysis were compared with those observed in the experiment in both Figs. 7 (a) and (b). They show very good coincidence. This fact implies that information supplied by the analysis is reliable and that the analysis can and will furnish information which could not be obtained by experiment.

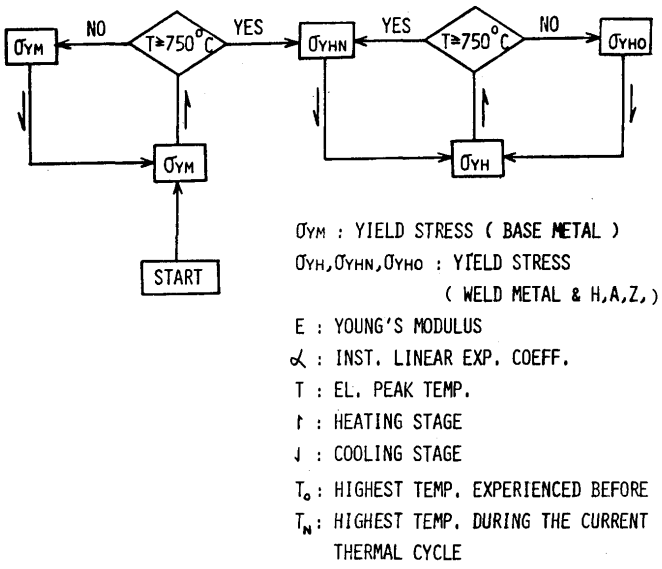

Fig. 5 (a). Mechanical properties of the metal.

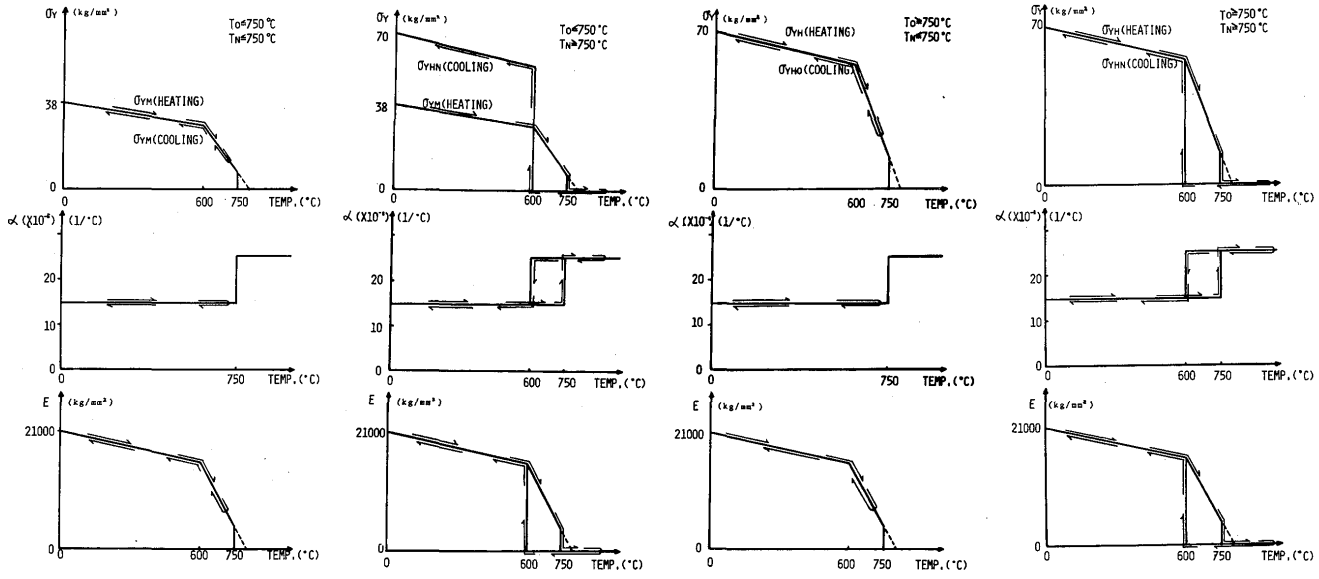

Fig. 5 (b). Mechanical properties of the metal.

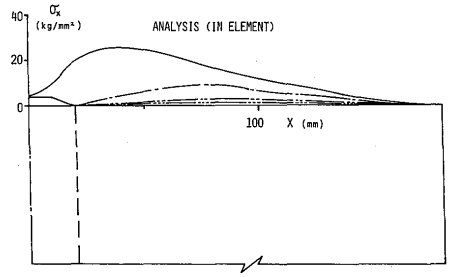

Fig. 6 (a). Longitudinal transient stresses on surface.

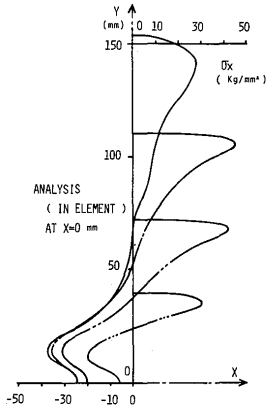

Fig. 6 (b). Longitudinal transient stresses in y-axis.

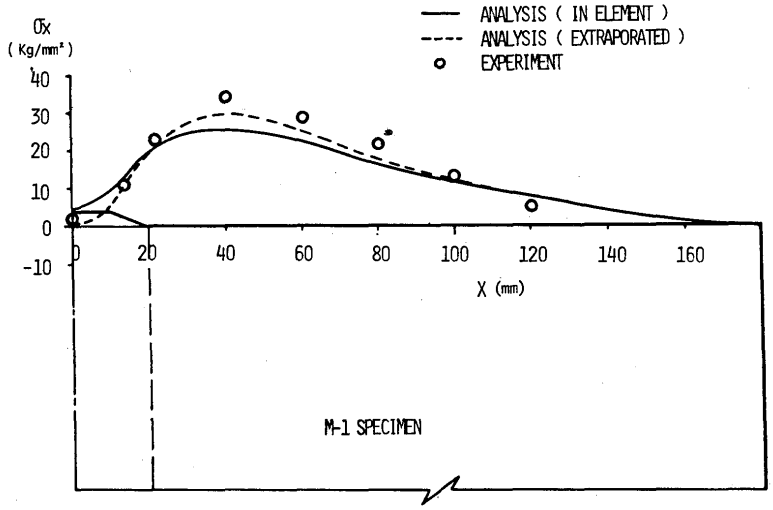

Fig. 7 (a). Longitudinal residual stresses on surface.

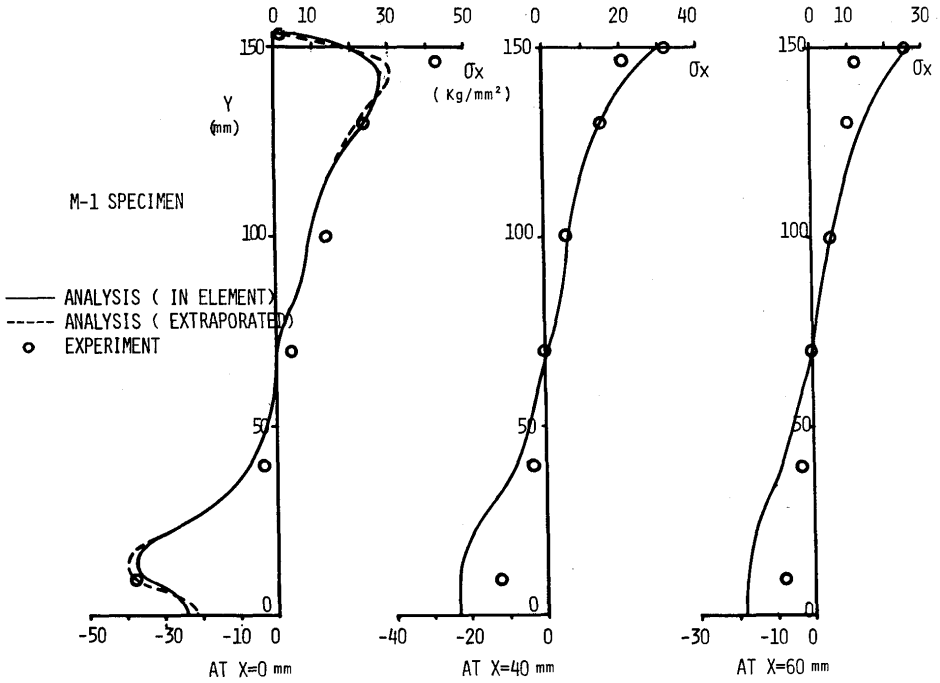

Fig. 7 (b). Longitudinal residual stresses in y-axis.

5. Concluding Remarks

The mechanical behavior of a multi-pass welded connection (167 passes) during welding including the resulting residual stresses, was investigated by means of the experiment and the theoretical analysis with the aid of the finite element method. In the study, the connection of a pressure vessel was idealized taking into account of the actual mechanical condition as much as possible.

From the results of the investigation, the following important information was obtained.

(1) The residual stresses predicted by the theoretical analysis coincide well with those obtained by the experiment. This implies that the analytical method applied is reliable even for this kind of very complicated problem, and can be expected to provide information which would not be readily obtained by experiment.

(2) The highest transient stress always appears below the surface of the latest layer, where it is comparatively small.

(3) In the residual longitudinal stress distribution, the location of the highest stress is several layers below the finishing bead in the midsection, and is about 20 mm away from the toe of the bead on the surface.

(4) Delayed cracking will initiate below the finishing bead and propagate to the surface.

Sincere appreciation is expressed to professor K. Satoh of Osaka University and Mr. T. Yamauchi, Manager of Kobe Steel Ltd. for their advices and suggestions throughout this investigation.

References

1) Satoh, K., Ueda, Y. and Kihara, H., "Recent Trend of Researches on Restraint Stresses and Strains for Weld Cracking", IIW Doc. X-659-72, IX-788-72, and Trans. of JWRI (Welding Research Institute of Osaka Univ., Japan) Vol. 1, No. 1, 1972, 53-68.

2) Ueda, Y. and Yamakawa, T., "Analysis of Thermal Elastic-Plastic Stress and Strain during Welding by Finite Element Method", IIW Doc. X-616-71, and Trans. of the Japan Welding Society, Vol. 2, No. 2, 1971, 90-100.

3) Ueda, Y. and Yamakawa, T., "Mechanical Characteristics of Cracking of Welded Joints, Proc. of The 1 st Int. Symp. of the Japan Welding Society, Tokyo, Nov. 1971, IC5·1-IC5·13.

4) Ueda, Y. and Kusachi, Y., "Theoretical Analysis of Local Stresses and Strains in RRC Test Specimens at Crack Initiation", IIW Doc. X-662-72.

5) Ueda, Y., Takahashi, E., Fukuda, K. and Nakacho, K., "Analysis of Thermal Elastic-Plastic Stresses and Strains due to Welding-Multilayer Welds" Proc. of National Symp. of Methods of Structural Analysis and Design, The Society of Steel Construction of Japan, 1973, 419-426 (in Japanese).

Appendix

Basic Theory of Elastic-Plastic Thermal Stress Analysis by Finite Element Method

1. Basic Theory of Thermal Stress Analysis

The basic concept of the finite element method is expressed simply such as a structure is regarded as an assembly of simple structural elements interconnected at a discrete number of nodal points, where the equilibrium and compatibility conditions are satisfied. Accordingly, the structure in consideration should be divided into a finite number of elements at the analysis such as triangular finite elements for plane stress or strain problems, or tetrahedral finite elements for three dimensional problems.

One of the typical finite elements in the continuum concerned is considered here and its mechanical behavior exhibited in a course of thermal history is represented in matrix forms in the following.

The internal displacements, $\{s\}$, are expressed in terms of displacement functions, $[M]$, and general coordinates, $\{\alpha\}$;

$$\{s\}=[M]\{\alpha\}. \tag{1}$$

The nodal displacements, $\{w\}$, are obtained merely by substituting the coordinates of the nodal points of the element into the displacement function,

$$\{w\}=[T]\{\alpha\}, \tag{2}$$

and rearranging Eq. (2) leads to

$$\{\alpha\}=[T]^{-1}\{w\}.$$

Then, the internal displacements are written in terms of the nodal displacements

$$\{s\}=[M][T]^{-1}\{w\}\equiv[A]\{w\}. \tag{3}$$

The strains, $\{\varepsilon\}$, in the element are given by appropriate differentiation of the internal displacements and shown below in the form of increments,

$$\{d\varepsilon\}\equiv[B]\{dw\}. \tag{4}$$

Accordingly, the increment of stresses in the element is, with an appropriate matrix $[D]$, the elasticity matrix $[D^e]$ or the plasticity matrix $[D^p]$,

$$\{d\sigma\}=[D]\{d\varepsilon\}. \tag{5}$$

When initial strains, $\{d\varepsilon_0\}$, exist, the stress increments yield

$$\{d\sigma\}=[D]\{d\varepsilon-d\varepsilon_0\}. \tag{6}$$

In cases where the initial strains are functions of temperature such as thermal strains, Eq. (6) is re-written, in terms of temperature increment, dT, where matrix $\{C\}$ will be discussed later, as

$$\{d\sigma\}=[D]\{d\varepsilon\}-\{C\}\,dT. \tag{7}$$

The finite elements in the continuum are interconnected at the nodal points, and for the analysis, the relationship between the increments of the nodal forces, $\{dF\}$, and the nodal displacements, $\{dw\}$, should be obtained. This will be followed by applying the principle of virtual works as

$$\begin{aligned}\{dF\}&=\int[B]^T[D]\{d\varepsilon\}d\,(\mathrm{vol})-\int[B]^T\{C\}dTd\,(\mathrm{vol})\\&\equiv[K]\{dw\}-\{dL\},\end{aligned} \tag{8}$$

where

$$[K]=\int[B]^T[D][B]d\,(\mathrm{vol}),$$

$$\{dL\}=\int[B]^T\{C\}dTd\,(\mathrm{vol}).$$

Here, $[K]$ is the stiffness matrix and $\{dL\}$ are nodal forces due to initial strains. The equilibrium state of the whole structure will be kept in satisfying the additional equilibrium conditions at each step of temperature increments which are composed of individual equilibrium equations at each node, that is,

$$\Sigma\{dF\}=\Sigma[K]\{dw\}-\Sigma\{dL\}. \tag{9}$$

When there is no external force acting at the nodes, the above equations are expressed in the simple form,

$$\Sigma\{dL\}=\Sigma[K]\{dw\}. \tag{10}$$

This is the basic equation for the analysis. With the lapse of time, the temperature distribution alters and its change produces thermal stress. In order to carry out the computation of the above equations for the given small changes in the temperature distribution, it is necessary to obtain $[K]$ and $\{dL\}$, which requires expressing $[D]$ and $\{C\}$ in Eq. (7) in explicit form, including effects of temperature on the material properties, as $[B]$ is obtained by simple differentiation of the selected displacement function of the finite element.

2. Stress and Strain Relation Influenced by Temperature

Mechanical properties of metals change under various conditions. When temperature increases, the modulus of elasticity, yield stress and rate of strain-hardening of the metal change. The plastic strain cycles of the metal cause Bauschinger's effect.

In the following, it is assumed that temperature only influences the modulus of elasticity, the yield stress and the rate of strain-hardening. The rate of thermal expansion is also dealt to depend upon temperature in the entire course of analysis. Furthermore, the influences of plastic strain rate and history can be taken into consideration for the stress and strain relation, if they can be expressed in some manageable forms of mathematical expression.

A. Stress-Strain Relation in Elastic Range

In the elastic range of the material, the total increments of strain consist of elastic strain increments $\{d\varepsilon^e\}$ and thermal expansion strain incremets $\{d\varepsilon^T\}$,

$$\{d\varepsilon\}=\{d\varepsilon^e\}+\{d\varepsilon^T\}. \tag{11}$$

The thermal (expansion) strains $\{d\varepsilon^T\}$ in the above expression, using $\{\alpha\}=\{\partial\varepsilon^T/\partial T\}$ as the instantaneous coefficient of linear expansion, are shown to be

$$\{d\varepsilon^T\}=\{\alpha\}dT. \tag{12}$$

When the elasticity matrix, $[D^e]$, changes as temperature increases, the strain increments $\{d\varepsilon^e\}$ are shown as

$$\begin{aligned}\{d\varepsilon^e\}&=[D^e]^{-1}\{d\sigma\}+\frac{\partial[D^e]^{-1}}{\partial T}\{\sigma\}dT\\&\equiv\{d\varepsilon^{e\prime}\}+\{d\varepsilon^{T\prime}\}.\end{aligned} \tag{13}$$

Solving the above equations, $\{d\sigma\}$ are given by

$$\{d\sigma\}=[D^e]\{d\varepsilon^e\}-[D^e]\frac{\partial[D^e]^{-1}}{\partial T}\{\sigma\}dT. \tag{14}$$

Substitution of Eqs. (11) and (12) into Eq. (14) becomes

$$\begin{aligned}\{d\sigma\}=[D^e]\{d\varepsilon\}-[D^e]\left(\{\alpha\}+\frac{\partial[D^e]^{-1}}{\partial T}\{\sigma\}\right)\\\times dT=[D^e]\{d\varepsilon^{e\prime}\}.\end{aligned} \tag{15}$$

Thus, in the case of elastic behavior, the required matrices $[D]$ and $\{C\}$ in Eq. (7) in the previous section, are obtained in the form

$$[D]=[D^e],\quad \{C\}=[D^e]\left(\{\alpha\}+\frac{\partial[D^e]^{-1}}{\partial T}\{\sigma\}\right). \tag{16}$$

B. Stress-Strain Relation in Plastic Range

Subjected to more loading, the material reaches the plastic range. At that instant, the stresses satisfy the condition

$$f(\sigma)=f_0(\varepsilon_p,\ T), \tag{17}$$

where f is the yield function and f_0 is a function of the yield stress which is influenced by the temperature and the plastic strain history. For the plastic strain increments, $\{d\varepsilon^p\}$, the material is assumed to be incompressible. According to the incremental

theory of plasticity, the plastic strain increments $\{d\varepsilon^p\}$ are given in the following form,

$$\{d\varepsilon^p\}=\lambda\left\{\frac{\partial f}{\partial\sigma}\right\}, \tag{18}$$

where f is regarded as plastic potential and λ is a positive value of scalar.

In this case, the total strain increments, $\{d\varepsilon\}$, are given as the summation of increments in elastic, plastic and thermal expansion strains, that

$$\{d\varepsilon\}=\{d\varepsilon^e\}+\{d\varepsilon^p\}+\{d\varepsilon^T\}. \tag{19}$$

Introduction of Eq. (13) into the above equation gives

$$\{d\varepsilon\}=\{d\varepsilon^{e'}\}+\{d\varepsilon^p\}+\{d\varepsilon^{T'}\}+\{d\varepsilon^T\}. \tag{20}$$

In the plastic range of the material under loading, the following condition should be satisfied:

$$\left\{\frac{\partial f}{\partial\sigma}\right\}^T\{d\sigma\}=\left\{\frac{\partial f_0}{\partial\varepsilon^p}\right\}^T\{d\varepsilon^p\}+\frac{\partial f_0}{\partial T}dT. \tag{21}$$

Similar to the previous section, the increments of stress $\{d\sigma\}$ are represented by a produce of the matrix $[D^e]$ and the elastic strain increment without the thermal expansion strains as

$$\{d\sigma\}=[D^e]\{d\varepsilon^{e'}\}. \tag{22}$$

From Eqs. (18), (20), (21), and (22), λ will be obtained as follows:

$$\lambda=\left[\left\{\frac{\partial f}{\partial\sigma}\right\}^T[D^e]\{d\varepsilon\}-\left\{\frac{\partial f}{\partial\sigma}\right\}^T[D^e]\left(\{\alpha\}+\frac{\partial[D^e]^{-1}}{\partial T}\{\sigma\}\right)dT-\frac{\partial f_0}{\partial T}dT\right]\times\left[\left\{\frac{\partial f}{\partial\sigma}\right\}^T[D^e]\left\{\frac{\partial f}{\partial\sigma}\right\}+\left\{\frac{\partial f_0}{\partial\varepsilon^p}\right\}^T\left\{\frac{\partial f}{\partial\sigma}\right\}\right]^{-1}. \tag{23}$$

These equations furnish the relation between the stress increments and total strain increments that is

$$\{d\sigma\}=[D^p]\{d\varepsilon\}-\left([D^p]\{\alpha\}+[D^p]\frac{\partial[D^e]^{-1}}{\partial T}\{\sigma\}+[D^e]\left\{\frac{\partial f}{\partial\sigma}\right\}\left(\frac{\partial f_0}{\partial T}\right)/S\right)dT, \tag{24}$$

where

$$[D^p]=[D^e]-[D^e]\left\{\frac{\partial f}{\partial\sigma}\right\}\left\{\frac{\partial f}{\partial\sigma}\right\}^T[D^e]/S, \tag{25}$$

$$S=\left\{\frac{\partial f}{\partial\sigma}\right\}^T[D^e]\left\{\frac{\partial f}{\partial\sigma}\right\}+\left\{\frac{\partial f_0}{\partial\varepsilon^p}\right\}^T\left\{\frac{\partial f}{\partial\sigma}\right\}. \tag{26}$$

Then, the required $[D]$ and $\{C\}$ matrices in Eq. (7) are shown to be

$$[D]=[D^p],$$

$$\{C\}=[D^p]\{\alpha\}+[D^p]\frac{\partial[D^e]^{-1}}{\partial T}\{\sigma\}+[D^e]\left\{\frac{\partial f}{\partial\sigma}\right\}\left(\frac{\partial f_0}{\partial T}\right)/S. \tag{27}$$

The matrix $[D^p]$ in the above is called plasticity matrix.

When λ is found to be negative during the process of computation, the material is subjected to unloading, that is,

$$\lambda<0. \tag{28}$$

Once unloading is detected, the stress-strain relation should be replaced by Eq. (15) instead of Eq. (24).

C. Basic Equations for Orthotropic and Isotropic Material

The basic theory in the preceding sections is applicable not only to isotropic but also to orthotropic material.

In order to perform the analysis, $[K]$ and $\{dL\}$ in Eq. (8) should be calculated. As $[B]$ is reduced by differentiation of the selected displacement functions, it is only necessary to show $[D]$ and $\{C\}$ matrices in Eq. (7), that is, stress-strain relation in both the elastic and plastic range of the material in explicit form.

The result of manipulation will be shown for orthotropic and isotropic material of strain hardening in this section.

In the elastic range of orthotropic material, the elasticity matrix is

$$[D^e]=\begin{pmatrix} d_{11} & d_{12} & d_{13} & 0 & 0 & 0\\ d_{21} & d_{22} & d_{23} & 0 & 0 & 0\\ d_{31} & d_{32} & d_{33} & 0 & 0 & 0\\ 0 & 0 & 0 & d_{44} & 0 & 0\\ 0 & 0 & 0 & 0 & d_{55} & 0\\ 0 & 0 & 0 & 0 & 0 & d_{66}\end{pmatrix}. \tag{29}$$

In the case of isotropic material, it becomes

$$[D^e]=\frac{E}{(1+\nu)(1-2\nu)}\times\begin{pmatrix} 1-\nu & \nu & \nu & 0 & 0 & 0\\ \nu & 1-\nu & \nu & 0 & 0 & 0\\ \nu & \nu & 1-\nu & 0 & 0 & 0\\ 0 & 0 & 0 & \frac{1-2\nu}{2} & 0 & 0\\ 0 & 0 & 0 & 0 & \frac{1-2\nu}{2} & 0\\ 0 & 0 & 0 & 0 & 0 & \frac{1-2\nu}{2}\end{pmatrix} \tag{30}$$

According to Hill's yield condition, the functions f and f_0 in Eq. (17) are expressed as

$$f=\bar{\sigma},\quad f_0=\sigma_0, \tag{31}$$

where

$$\bar{\sigma}^2=\frac{3}{2(F+G+H)}[F(\sigma_y-\sigma_z)^2+G(\sigma_z-\sigma_x)^2 +H(\sigma_x-\sigma_y)^2+2L\tau_{yz}^2+2M\tau_{zx}^2+2N\tau_{xy}^2]. \tag{32}$$

In the above expression $\bar{\sigma}$ and σ_0 are the equivalent stress and the yield stress, respectively, and F, G, H, L, M, and N are parameters indicating the orthotropy. For the case of isotropic material, the basic equations are obtained by only substituting the following relation

$$3F=3G=3H=L=M=N \tag{33}$$

into the above Eq. (32), and the results of manipulation are the following.

In the plastic range of the material, the rate of strain-hardening, H', is defined as

$$H'=d\bar{\sigma}/d\bar{\varepsilon}^p, \tag{34}$$

where

$$(d\bar{\varepsilon}^p)^2=\frac{2}{3}(F+G+H) \times\left[\frac{F(Gd\varepsilon_y^p-Hd\varepsilon_z^p)^2+G(Hd\varepsilon_z^p-Fd\varepsilon_x^p)^2+H(Fd\varepsilon_x^p-Gd\varepsilon_y^p)}{(FG+GH+HF)^2} +\frac{(d\gamma_{yz}^p)^2}{2L}+\frac{(d\gamma_{zx}^p)^2}{2M}+\frac{(d\gamma_{xy}^p)^2}{2N}\right], \tag{35}$$

and λ is calculated by the equation in the form of

$$\lambda=\frac{1}{3S}\{S_1d\varepsilon_x+S_2d\varepsilon_y+S_3d\varepsilon_z+S_4d\gamma_{yz}+S_5d\gamma_{zx}+S_6d\gamma_{xy} +(S_1'\varepsilon_x^e+S_2'\varepsilon_y^e+S_3'\varepsilon_z^e+S_4'\gamma_{yz}^e+S_5'\gamma_{zx}^e+S_6'\gamma_{xy}^e)dT -(S_1\alpha_x+S_2\alpha_y+S_3\alpha_z)dT-\frac{2}{3}\sigma_0\frac{d\sigma_0}{dT}dT\}, \tag{36}$$

where

$$S=\frac{4}{9}\bar{\sigma}^2H+S_1\sigma_x'+S_2\sigma_y'+S_3\sigma_z'+2S_4\tau_{yz}'+2S_5\tau_{zx}'+2S_6\tau_{xy}',$$

$$S_1=d_{11}\sigma_x'+d_{12}\sigma_y'+d_{13}\sigma_z',\qquad S_4=2d_{44}\tau_{yz}',$$
$$S_2=d_{21}\sigma_x'+d_{22}\sigma_y'+d_{23}\sigma_z',\qquad S_5=2d_{55}\tau_{zx}',$$
$$S_3=d_{31}\sigma_x'+d_{32}\sigma_y'+d_{33}\sigma_z',\qquad S_6=2d_{66}\tau_{xy}',$$
$$\sigma_x'=\frac{H(\sigma_x-\sigma_y)+G(\sigma_x-\sigma_z)}{F+G+H},\qquad \tau_{yz}'=\frac{L\tau_{yz}}{F+G+H},$$
$$\sigma_y'=\frac{F(\sigma_y-\sigma_z)+H(\sigma_y-\sigma_x)}{F+G+H},\qquad \tau_{zx}'=\frac{M\tau_{zx}}{F+G+H},$$
$$\sigma_z'=\frac{G(\sigma_z-\sigma_x)+F(\sigma_z-\sigma_y)}{F+G+H},\qquad \tau_{xy}'=\frac{N\tau_{xy}}{F+G+H},$$
$$S_1'=\frac{\partial S_1}{\partial T},\ S_2'=\frac{\partial S_2}{\partial T},\ S_3'=\frac{\partial S_3}{\partial T},\ S_4'=\frac{\partial S_4}{\partial T},$$
$$S_5'=\frac{\partial S_5}{\partial T},\ S_6'=\frac{\partial S_6}{\partial T},$$
$$\{\varepsilon_x^e,\ \varepsilon_y^e,\ \varepsilon_z^e,\ \gamma_{yz}^e,\ \gamma_{zx}^e,\ \gamma_{xy}^e\}^T=[D^e]^{-1}\{\sigma\}.$$

With these notations, the plasticity matrix $[D^p]$ is written as

$$[D^p]=[D^e]-\frac{1}{S}\begin{pmatrix} S_1^2 & S_1S_2 & S_1S_3 & S_1S_4 & S_1S_5 & S_1S_6\\ & S_2S_2 & S_2S_3 & S_2S_4 & S_2S_5 & S_2S_6\\ & & S_3S_3 & S_3S_4 & S_3S_5 & S_3S_6\\ & \text{SYM} & & S_4S_4 & S_4S_5 & S_4S_6\\ & & & & S_5S_5 & S_5S_6\\ & & & & & S_6S_6 \end{pmatrix} \tag{37}$$

The last term which appears in Eq. (27) in the matrix $\{C\}$ is represented as

$$[D^e]\left\{\frac{\partial f}{\partial\sigma}\right\}\left(\frac{\partial f_0}{\partial T}\right)\Big/S=\frac{2\sigma_0}{3S}[S_1,\ S_2,\ S_3,\ S_4,\ S_5,\ S_6]^T\frac{\partial\sigma_0}{\partial T} \tag{38}$$